

1 Wireless signals¹

Before we embark on a discussion of the characterization and modeling of nonlinear RF devices and circuits, let us review the attributes of their customers, the RF signals used in wireless communication. In this chapter, we will briefly discuss the trends of wireless communication systems and standards for cellular networks, wireless local area networks (WLANs), and wireless metropolitan networks (WMANs) and the challenges they create in the development of low-cost, linear, and power-efficient RF electronics. Various metrics used to characterize signals and systems will then be introduced.

1.1 Modern wireless communications

Wireless communication systems rely on the modulation of radio-frequency signals to exchange information. In modern wireless communication, digital modulation techniques whereby the digital information is encoded using amplitude (ASK), phase (PSK) or frequency (FSK) shift keying are used. In the most general case, quadrature amplitude modulation (QAM), whereby the amplitude $A(t)$ and phase $\phi(t)$ of the RF waves are both modulated, is used:

$$\begin{aligned} x_{\text{RF}}(t) &= A(t)\cos[\omega_{\text{RF}}t + \phi(t)] \\ &= I(t)\cos(\omega_{\text{RF}}t) - Q(t)\sin(\omega_{\text{RF}}t). \end{aligned}$$

In the above equation, $I(t)$ and $Q(t)$ represent the in-phase and quadrature components of the modulation, respectively.

It is to be noted that constant-envelope signals ($I^2(t) + Q^2(t) = \text{constant}$) are advantageous for mobile transmitters because they can then be amplified by nonlinear power amplifiers, without AM-to-PM distortions degrading the modulation of the signals transmitted. Such nonlinear amplifiers have the advantage of being both cheaper and more power-efficient than linear amplifiers.

Phase modulation is then attractive if it can be implemented in such a way that the phase-modulated signals can maintain their constant envelope $A^2 = I^2(t) + Q^2(t)$ while being processed by bandpass-limited circuits. One modulation scheme, GMSK (Gaussian minimum shift keying) [1], achieves this ability via the use of gradual

¹ Research collaboration with Jiwoo Kim and Suk Keun Myoung is gratefully acknowledged.

phase transition, which greatly helps maintain the signal envelope constant. The quasi-constant envelope of GMSK is beneficially used in wireless standards such as the GSM (Global System for Mobile Communication). The resulting low cost and power efficiency of the mobiles certainly contributed to the widespread success of this protocol around the world.

Nevertheless, given the needs to increase the wireless network’s capacity to handle more users and to provide wide-bandwidth data services, digital quadrature amplitude modulation is becoming more prevalently used in modern standards.

Beside the modulation of the RF signals to encode information, the multiple division access (MDA) scheme used to handle multiple users or to increase the bandwidth for a single user is also of great importance. As symbolically represented in Figure 1.1, frequency (FDMA), time (TDMA), and code (CDMA) division multiple-access techniques are typically used to handle multiple users [1]. In CDMA, each user baseband signal is further modulated by a pseudonoise code with high chip-rate which spreads the bandwidth of the original baseband signal. Clearly CDMA calls for mobiles with front ends operating with wider frequency bandwidth.

Note that often the uplink and downlink between the mobile and the basestations use different frequencies, therefore relying on frequency-division duplexing. Alternatively, time-division duplexing (transmit and receive at different times) is used when the same frequency band is used.

In addition, the concept of the cellular network provides a frequency reuse in non-adjacent cells, which increases the capacity. Space-division multiplexing access (SDMA), or the use of antennas with beam-forming techniques, also enables further increase of the user capacity by adding additional sectors in each cell.

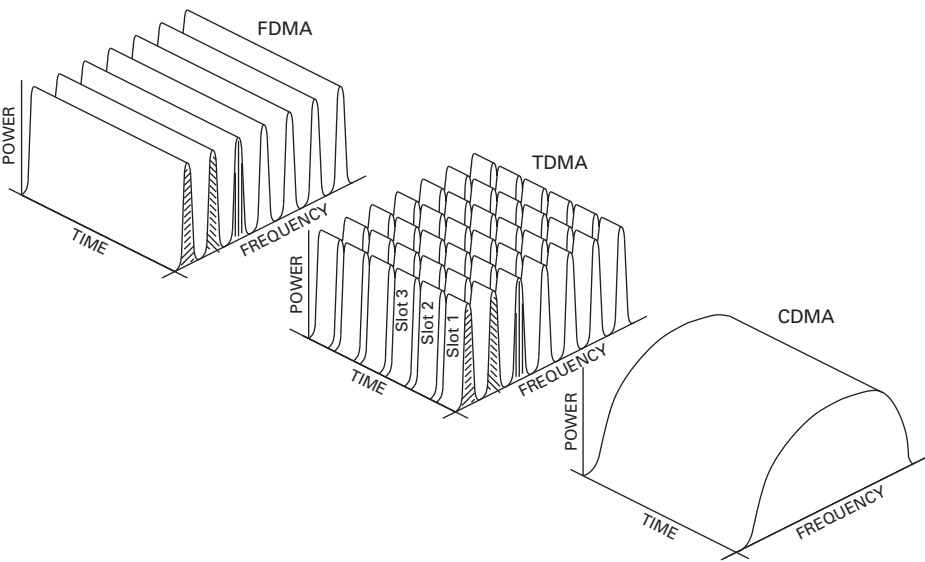


Figure 1.1 Comparison of FDMA, TDMA, and CDMA schemes.

Unlike the mobiles which in TDMA and FDMA handle a single channel, the power amplifiers at the basestation transmitter must typically operate with much wider bandwidth because it is more economical to use a single basestation RF power amplifier for the various channels for each RF carrier. Furthermore, basestation power amplifiers typically handle multiple carriers at the same time. This obviously introduces some critical constraints upon the linearity and bandwidth of these power amplifiers.

One of the motivations for the introduction of CDMA was its improved performance in handling fading (signal cancellation arising from multi-path propagation), owing to its wider bandwidth. CDMA can also make beneficial use of the various multi-path signals using a “rake receiver” [1] to reduce the signal-to-noise ratio at the output. Another division multiplexing technique that has gained prevalence in wireless communication systems due to its high performance in multi-path environments is OFDMA (orthogonal frequency-division multiplex access). OFDMA is a multi-user version of OFDM (orthogonal frequency-division multiplexing), which is used in high-performance WiFi WLANs, and is now being actively implemented in new WMAN standards such as WiMAX and LTE to provide wide-bandwidth data services [2] [3] [4]. Given the rapid growth in this field, we will discuss the characteristics of OFDM signals in the next section. The analysis of OFDM signals will also illustrate the challenges modern modulation schemes place upon the characterization and design of modern RF circuits.

1.2 OFDM primer

In this section we shall give a brief review of the most salient features of OFDM. OFDM signals typically consist of multiple symbols separated by a guard interval. The general structure of an idealized OFDM symbol of duration T_{SYMB} is shown in Figure 1.2, where $W_{T,\text{SYMB}}(t)$ is an ideal shaping window.

The symbol duration is given by $T_{\text{SYMB}} = T_{\text{IFFT}} + T_{\text{GI}} + T_{\text{TR}}$ with T_{GI} the guard interval and T_{TR} the transition interval. The guard interval T_{GI} and the associated cyclic prefix $T_{\text{CP}} = T_{\text{GI}} + T_{\text{TR}}$ are used to remove the intersymbol interference (ISI) from symbol to symbol as well as to maintain the subcarrier orthogonality in each symbol as we shall discuss below. The transition interval T_{TR} , which is not always specified in

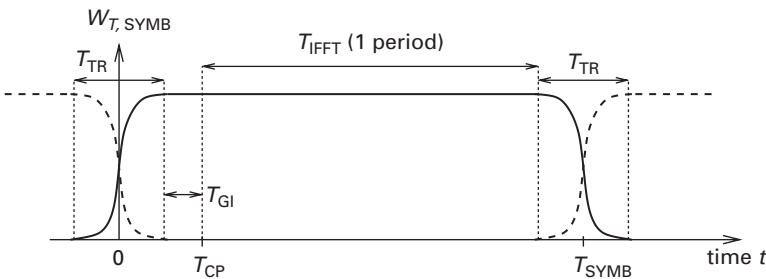


Figure 1.2 Structure of an OFDM symbol of duration T_{SYMB} .

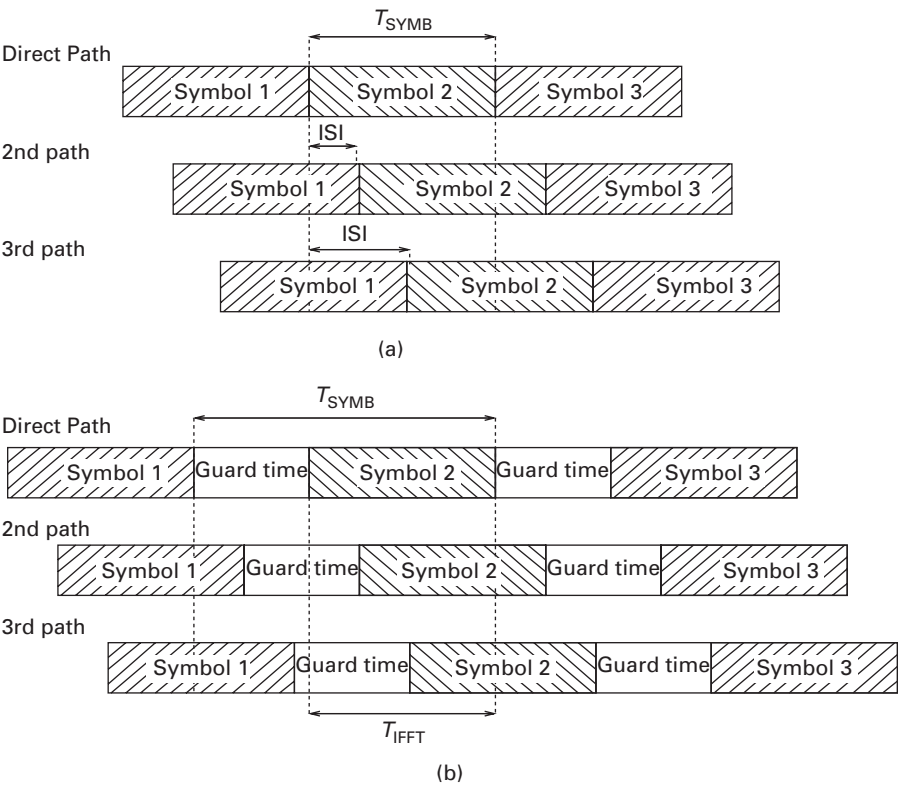


Figure 1.3 The ISI shown to take place in (a) is suppressed in (b) by the use of a guard interval between symbols.

the standards, is used to reduce the spectral regrowth associated with the transition from one to another symbol.

The use of the guard interval is illustrated in Figure 1.3. The intersymbol interference is suppressed if the guard time is larger than the channel delay spread. However, self-interference in a given symbol still needs mitigation, and this will be discussed later on.

Let us consider now a single OFDM symbol with index k . The data portion $x_{\text{RF},k}$ which is located in the interval $kT_{\text{SYMB}} + [T_{\text{CP}}, T_{\text{CP}} + T_{\text{IFFT}}]$ is of the form

$$x_{\text{RF}}(t) = \text{Re} \left\{ \sum_k x_k(t - kT_{\text{SYMB}}) \exp[j2\pi f_0 t] \right\},$$
$$x_k(t) = \text{rect} \left(\frac{t - (T_{\text{CP}} + T_{\text{IFFT}}/2)}{T_{\text{IFFT}}} \right) \sum_{n=1}^{N_{\text{SC}}} C_{k,n} \exp[j2\pi n \Delta f (t - T_{\text{CP}})].$$

The Fourier transform $X_k(f) = \mathcal{F}[x_k]$ associated with the symbol x_k is

$$X_k(f) = T_{\text{IFFT}} \sum_{n=1}^{N_{\text{SC}}} C_{k,n} \exp[-j2\pi n \Delta f (2T_{\text{CP}} + T_{\text{IFFT}}/2)] \times \text{sinc} \left(\frac{f - n \Delta f}{\Delta f} \right).$$

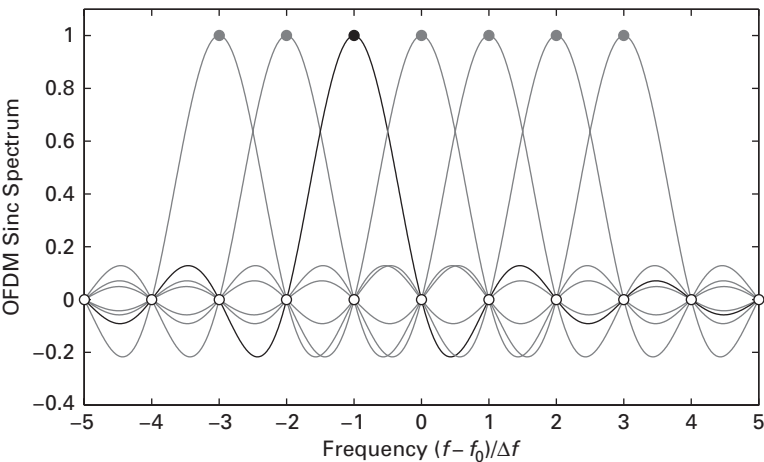


Figure 1.4 Normalized spectrum for seven adjacent subcarriers of an OFDM signal with subcarrier # -1 highlighted.

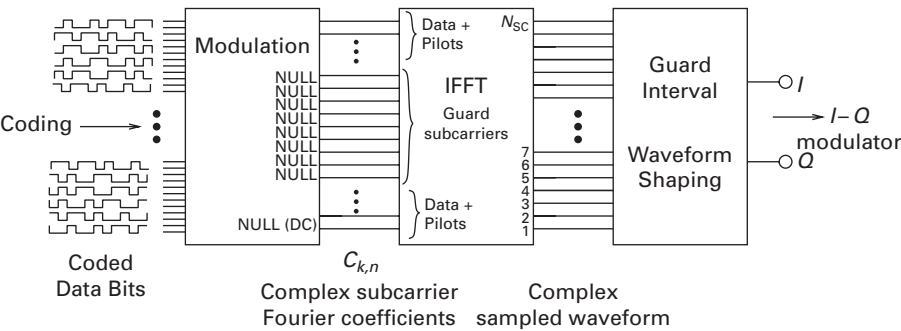


Figure 1.5 Transmitter implementation using IFFT.

The spectrum of the OFDM signal is obtained from the coherent superposition of the individual spectra of the various subcarriers. As can be seen in Figure 1.4, the spectra of the various subcarriers overlap in most of the frequency range. However, if we sample the frequency at $n \Delta f = n / T_{\text{IFFT}}$, the spectra are orthogonal. This frequency sampling is equivalent to assuming that the signal $x_k(t)$ is a periodic function of time t with period T_{IFFT} . The orthogonality in OFDM is then achieved by selecting $T_{\text{IFFT}} = 1/\Delta f$. The coefficients $C_{k,n}$ can then be recovered by performing a Fourier series over the data interval $kT_{\text{SYMB}} + [T_{\text{CP}}, T_{\text{CP}} + T_{\text{IFFT}}]$. For sampled data, a Fourier series is exactly implemented (up to the scaling factor N_{IFFT}) by a fast Fourier transform (FFT) performed using N_{SC} data acquired during the data interval. Conversely, the sampled signal $x_k(nT_s)$ can be generated by an inverse FFT (IFFT) as indicated in Figure 1.5.

The complex Fourier coefficients C_k are typically generated using BPSK, QPSK, 16-QAM or 64-QAM modulation:

$$C_{k,n} = (I_{k,n} + jQ_{k,n}) \times K_{\text{MOD},k},$$

Table 1.1. Parameters for WiFi, WiMAX (downlink), and LTE (downlink) for their widest-bandwidth configuration. Note that different circular prefixes (normal/extended) are used in LTE depending on the channel delay spread and the environment (urban/rural).

	WiFi 802.11a	WiMAX 806.16e-2005	LTE
Bandwidth	20 MHz	20 MHz	20 MHz
Number of subcarriers (N_{SC})	64	2048	2048
Number of data subcarriers	48	1440	1200
Number of null subcarriers	12	368	
Number of pilot subcarriers	4	240	
Subcarrier frequency (Δf)	0.3125 MHz	10.94 kHz	15 kHz
IFFT period ($T_{IFFT} = 1/\Delta f$)	3.2 μs	91.41 μs	66.67 μs
Circular prefix (T_{CP})	0.8 μs	11.4 μs	5/16.67 μs
Ratio T_{CP}/T_{IFFT}	1/4	1/8	1/14–1/4
Symbol interval (T_{SYMB})	4.0 μs	102.9 μs	71.67/183.34 μs

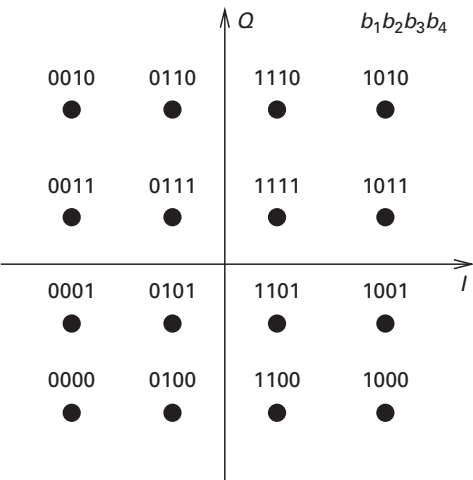


Figure 1.6 A 16-QAM constellation with Gray coding.

where K_{MOD} is a constant depending on the modulation used and the output power to be generated. An example of a 16-QAM constellation with Gray digital encoding is shown in Figure 1.6. Typical values found for the various OFDM parameters in various standards are shown in Table 1.1.

Let us discuss now how the self-interference in a given symbol is mitigated in the presence of multi-path signals. Orthogonality between the subcarriers is preserved if the symbols are periodically extended inside the guard interval time. This is symbolically represented in Figure 1.7 for the case of the reception of a symbol with three different propagation delays. In the useful symbol interval of duration T_{IFFT} , the various path delays only introduce a frequency-dependent phase shift and amplitude rescaling in

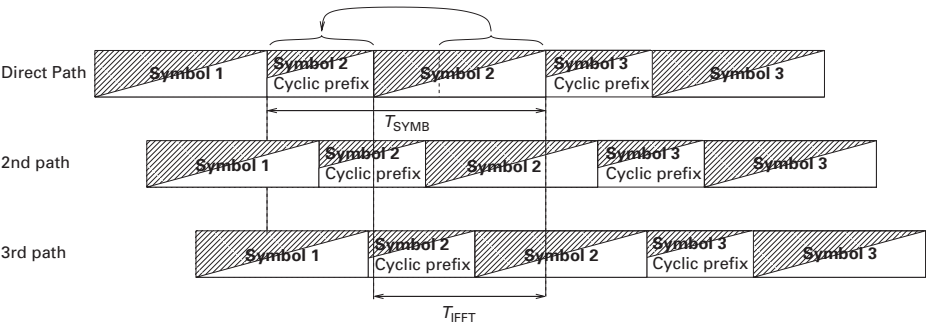


Figure 1.7 Use of a cyclic prefix to mitigate multi-path propagation.

each of the measured subcarriers which can be removed by subsequent processing at the receiver.

Having presented the fundamentals of the OFDM scheme, let us now discuss its signal characteristics. OFDM signals exhibit a very high peak-to-average power ratio (PAPR),

$$\text{PAPR} = \frac{P_{\text{peak}}}{P_{\text{avg}}}.$$

This is due to the fact that OFDM signals are realized as the superposition of multiple subcarriers N_{SC} , and there exists a finite probability that at some times all these subcarriers can be in phase. Under such a circumstance the peak power is proportional to N_{SC}^2 . Since the average power is proportional to N_{SC} , assuming all subcarriers have the same power, it results that at these fleeting times the PAPR reaches N_{SC} , which can be very large, e.g. 2048 (33 dB). Such a PAPR would be quite alarming. However, the probability of such an event is small, since it is proportional to $2^{-N_{\text{SC}}}$.

Let us introduce an instantaneous PAPR(t) in a time interval $[t, t + \Delta t]$ defined as

$$\text{PAPR}(t) = \frac{\max_{[t, t+\Delta t]} [|x_{\text{RF}}(t)|^2]}{E[|x_{\text{RF}}(t)|^2]},$$

with $E[\]$ the average operator taken over the transmit time interval of interest. It is possible to estimate the PAPR at the baseband signal level. We call $x(n)$ the complex baseband signal, which is defined as

$$x(n) = I(n) + jQ(n),$$

where the signals $I(n) = I(t_n)$ and $Q(n) = Q(t_n)$ are sampled at discrete time intervals $t_n = nt_s$ with t_s the sampling interval:

$$x_{\text{RF}}(t) = I(t)\cos(\omega_{\text{RF}}t) - Q(t)\sin(\omega_{\text{RF}}t).$$

The instantaneous PAPR at the sampling time t_n is then defined by

$$\text{PAPR}(n) = \frac{|x(n)|^2}{E[|x(n)|^2]} = \frac{I^2(n) + Q^2(n)}{E_{\text{avg}}} = \frac{P(n)}{P_{\text{avg}}},$$

where the average $E[\cdot]$ is taken over the transmitted data sequence. Note that E_{avg} is the average envelope value, $P(n)$ the discrete-time instantaneous RF power at time t_n , and P_{avg} the average RF power. Note that the instantaneous RF power $P(n)$ is simply obtained from the envelope $E(n) = |x(n)|$ using

$$P(n) = \frac{1}{2}|x(n)|^2 = \frac{1}{2}\left[I^2(n) + Q^2(n)\right] = \frac{1}{2}E^2(n).$$

Since the OFDM data can be assumed to be stochastically time-varying, the PAPR is best represented by its statistical distribution. It is common practice to use the complementary cumulative distribution function (CCDF = 1 – CDF) of the PAPR to represent its statistical distribution:

$$\text{CCDF(PAPR)} = \text{Probability}[P(n) > P_{\text{avg}} \times \text{PAPR}].$$

A simple and useful approximation for the CCDF has been proposed for QPSK OFDM [5]:

$$\text{CCDF(PAPR)} = 1 - \text{CDF} = 1 - \left[1 - \exp(-\text{PAPR})\right]^{\beta N_{\text{SC}}},$$

where the factor β is a fitting parameter used to approximate the oversampling factor. Note that $\beta = 1$ corresponds to the case of a Nyquist sampled signal. In such a Nyquist limit, by virtue of the central limit theorem, the samples $x_k(n)$ for each subcarrier can be assumed, for a large number N_{SC} of subcarriers, to be zero-mean Gaussian complex variables $N(0, \sigma^2)$ with variance σ . It results that $|x_{\text{OFDM}}(n)|$ is a Rayleigh distribution (Rayleigh[σ]) and the instantaneous power $|x_{\text{OFDM}}(n)|^2$ is exponentially distributed with mean power $\sigma_{\text{OFDM}}^2 = 2\sigma^2$. In the case of oversampling, the adjacent samples $x(n)$ are correlated, and a non-unity β factor ($\beta = 2.8$) is found to provide a correction to the correlation [5]. The results obtained for various numbers of subcarriers are shown in Figure 1.8. The larger the number of subcarriers, the larger the probability of obtaining a specific PAPR.

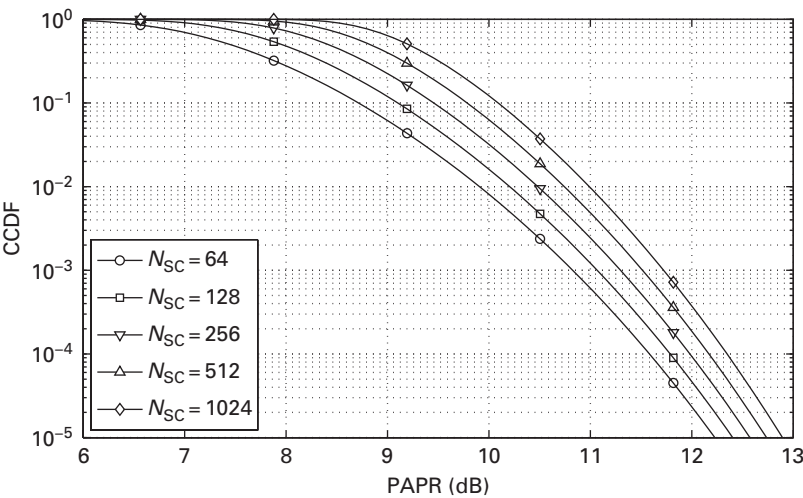


Figure 1.8 Approximate CCDF of PAPR for QPSK OFDM signals.

Note, however, that the discrete-time PAPR may underestimate the continuous-time PAPR since it is calculated using sampled data, but it nonetheless gives a useful lower-bound estimate of the analog PAPR which the amplifier must handle.

1.3 Impact of clipping on OFDM

As we have seen in the previous section, OFDM signals, just like CDMA signals, exhibit large PAPR. The question arises as to whether the peaks in the signal envelope carry critical modulation information and whether we could clip them off without significantly degrading the information transferred.

In hard clipping, the input signal $x(n) = I_{in}(n) + jQ_{in}(n)$ will have its envelope $|x(n)| = \sqrt{I_{in}^2(n) + Q_{in}^2(n)}$ rescaled to E_{clip} if the envelope exceeds the clipping threshold E_{clip} . However, this envelope clipping is performed in such a way as to maintain the phase $\angle(I_{in} + jQ_{in})$ information of the input signal. The output signal $y(n) = I_{out}(n) + jQ_{out}(n)$ will therefore be given by

$$I_{out}(n) = \text{Re}[x(n)] = \frac{E_{clip}}{|x(n)|} I_{in}(n),$$
$$Q_{out}(n) = \text{Im}[x(n)] = \frac{E_{clip}}{|x(n)|} Q_{in}(n).$$

Note that the output phase satisfies $\angle(I_{out} + jQ_{out}) = \angle(I_{in} + jQ_{in})$. Figure 1.9(a) shows a processing block that conceptually implements this hard-clipping function using an antipeak generator. The output signal $y(n) = x(n) + c(n)$ is the superposition of the incident signal x_{in} and a corrective clipping signal $c(n)$ generated by the antipeak generator:

$$c(n) = I_C + jQ_C = (I_{out} - I_{in}) + j(Q_{out} - Q_{in}).$$

The clipping ratio γ is defined as

$$\gamma = \frac{E_{clip}}{\sqrt{E[|x(n)|^2]}} = \frac{E_{clip}}{E_{avg}} = \sqrt{\frac{P_{clip}}{P_{avg}}},$$

where for OFDM signals the average power is $P_{avg} = \sigma_{OFDM}^2$.

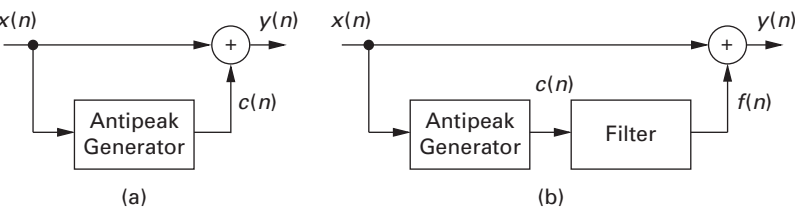


Figure 1.9 System diagrams for implementing hard clipping (a) and soft clipping (b).

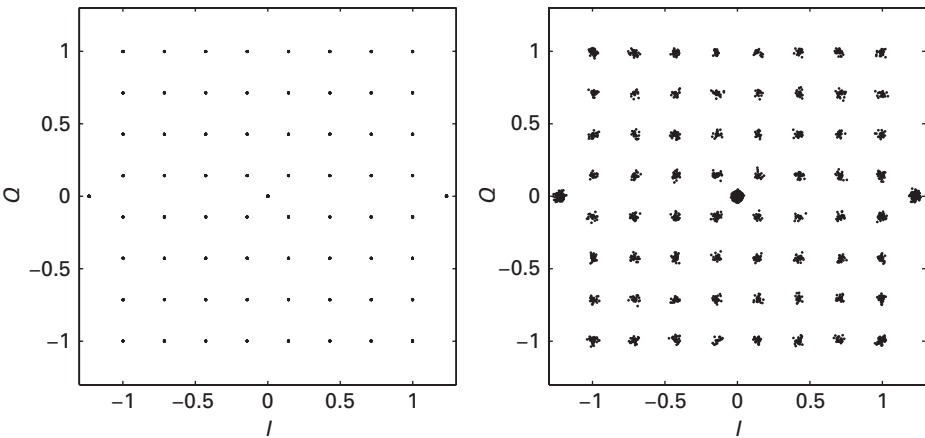


Figure 1.10 Constellation for the various OFDM subcarriers before (left) and after (right) hard clipping with a clipping level of 7 dB.

Hard clipping distorts the OFDM signals and generates both out-of-band spectral regrowth and in-band distortion. Let us first consider the in-band distortion. The distortion of the constellation in 64-QAM OFDM is shown in Figure 1.10. Clipping is seen to have introduced noise. Although the corrective signal $c(n)$ is clearly correlated to the input signal x_{in} , it has been demonstrated [6] [7] that for OFDM signals with a large number of subcarriers the clipped signal can be well represented by the superposition of an attenuated version of the input signal $\alpha x(n)$ and an uncorrelated additive noise $d(n)$:

$$y(n) = \alpha x(n) + d(n),$$

with α given by

$$\alpha = 1 - \exp(-\gamma^2) + \frac{\sqrt{\pi}}{2} \gamma \operatorname{erfc}[\gamma].$$

Figure 1.11 shows the variation of the attenuation constant α with the clipping ratio γ . For clipping ratios above 7 dB, the attenuation constant α is close to unity and can safely be neglected.

The uncorrelated additive noise $d(n)$ has been demonstrated [7] to have a variance given by

$$\sigma_d^2 = \sigma_{\text{OFDM}}^2 \left(1 - e^{-\gamma^2} - \alpha^2 \right).$$

The bit error probability (BEP) for M -QAM OFDM under clipping has been derived [7] to be given by

$$\text{BEP}_{\text{OFDM}} = \frac{2}{\log_2(M)} \left(1 - \frac{1}{\sqrt{M}} \right) \operatorname{erfc} \left[\frac{3 \times \text{SNDR}}{2(M-1)} \right],$$

with $\log_2(M)$ the number of bits in each M -ary-QAM subcarrier. In the expression for the BEP, SNDR is the signal-to-noise-plus-distortion ratio: